Inhalation Toxicology

http://tandfonline.com/iiht
ISSN: 0895-8378 (print), 1091-7691 (electronic)

Inhal Toxicol, 2016; 28(11): 520–535
 DOI: 10.1080/08958378.2016.1214768

Taylor & Francis
Taylor & Francis Group

RESEARCH ARTICLE

Predicting lung dosimetry of inhaled particleborne benzo[a]pyrene using physiologically based pharmacokinetic modeling

Jerry Campbell[1], Allison Franzen[2], Cynthia Van Landingham[2], Michael Lumpkin[3], Susan Crowell[4], Clive Meredith[5], Anne Loccisano[6], Robinan Gentry[2], and Harvey Clewell[1]

[1]Ramboll Environ, Research Triangle Park, NC, USA, [2]Ramboll Environ, Monroe, LA, USA, [3]ENVIRON International Corporation, Monroe, LA, USA, [4]Pacific Northwest National Laboratory, Richland, WA, USA, [5]British American Tobacco, GR&D, Southampton, United Kingdom of Great Britain and Northern Ireland, and [6]R.J. Reynolds Tobacco Company, Alexandria, VA, USA

Abstract

Benzo[a]pyrene (BaP) is a by-product of incomplete combustion of fossil fuels and plant/wood products, including tobacco. A physiologically based pharmacokinetic (PBPK) model for BaP for the rat was extended to simulate inhalation exposures to BaP in rats and humans including particle deposition and dissolution of absorbed BaP and renal elimination of 3-hydroxy benzo[a]pyrene (3-OH BaP) in humans. The clearance of particle-associated BaP from lung based on existing data in rats and dogs suggest that the process is bi-phasic. An initial rapid clearance was represented by BaP released from particles followed by a slower first-order clearance that follows particle kinetics. Parameter values for BaP-particle dissociation were estimated using inhalation data from isolated/ventilated/perfused rat lungs and optimized in the extended inhalation model using available rat data. Simulations of acute inhalation exposures in rats identified specific data needs including systemic elimination of BaP metabolites, diffusion-limited transfer rates of BaP from lung tissue to blood and the quantitative role of macrophage-mediated and ciliated clearance mechanisms. The updated BaP model provides very good prediction of the urinary 3-OH BaP concentrations and the relative difference between measured 3-OH BaP in nonsmokers versus smokers. This PBPK model for inhaled BaP is a preliminary tool for quantifying lung BaP dosimetry in rat and humans and was used to prioritize data needs that would provide significant model refinement and robust internal dosimetry capabilities.

Keywords

Benzo[a]pyrene, human dosimetry, lung deposition, particle inhalation, physiologically based pharmacokinetic model

History

Received 15 April 2016
Revised 1 July 2016
Accepted 14 July 2016
Published online 25 August 2016

Introduction

Benzo[a]pyrene (BaP) is a polycyclic aromatic hydrocarbon (PAH) found in automotive exhaust, coal tar, charbroiled meat, and as an incomplete combustion by-product of forest fires, burning fuels (wood, coal, petroleum products) and tobacco (USEPA, 2013). It is highly lipophilic, nonvolatile and typically considered to be a compound representative of the PAHs (Gerde et al., 2001). Tumors in the upper respiratory and gastrointestinal (GI) tracts of hamsters have been observed following inhalation exposure to BaP (Thyssen et al., 1981). BaP has been proposed to be carcinogenic to humans (Group 1 IARC classification) as well, although human epidemiological data for BaP inhalation exposures independent of other PAH exposures are not available (USEPA, 2013).

The nonvolatile nature of BaP emitted from wood/fuel or tobacco combustion increases the number of physical factors that must be taken into account to accurately describe BaP inhalation pharmacokinetics. Environmental inhalation exposures would not be to predominately BaP gas or pure BaP aerosols, but to BaP condensed onto carbonaceous carrier particle condensates (Pankow, 2001). Thus, the fractional deposition of BaP in the lungs and upper respiratory tract (URT) is determined by the physical characteristics of the carrier particles and breathing rates. Further, the strength of interaction of the BaP coating on the carrier particles and rate of dissolution of the BaP coating determines the extent and rate of BaP dissociation from the carrier particle (Gerde et al., 2001). The rate of diffusivity of BaP across the various lung epithelia and the presence of BaP-metabolizing enzymes in the lung epithelium may influence the amount of parent compound and metabolites that are available for lung tissue interaction or transport into the arterial blood (Gerde et al., 2001). Because BaP enters the airways and lung as a coating on a carrier particle, inhalation dosimetry must consider factors that are not typically

Address for correspondence: Allison Franzen, Ramboll Environ, Monroe, 6 Davis Drive, Research Triangle Park, North Carolina, 32709, USA. E-mail: afranzen@ramboll.com

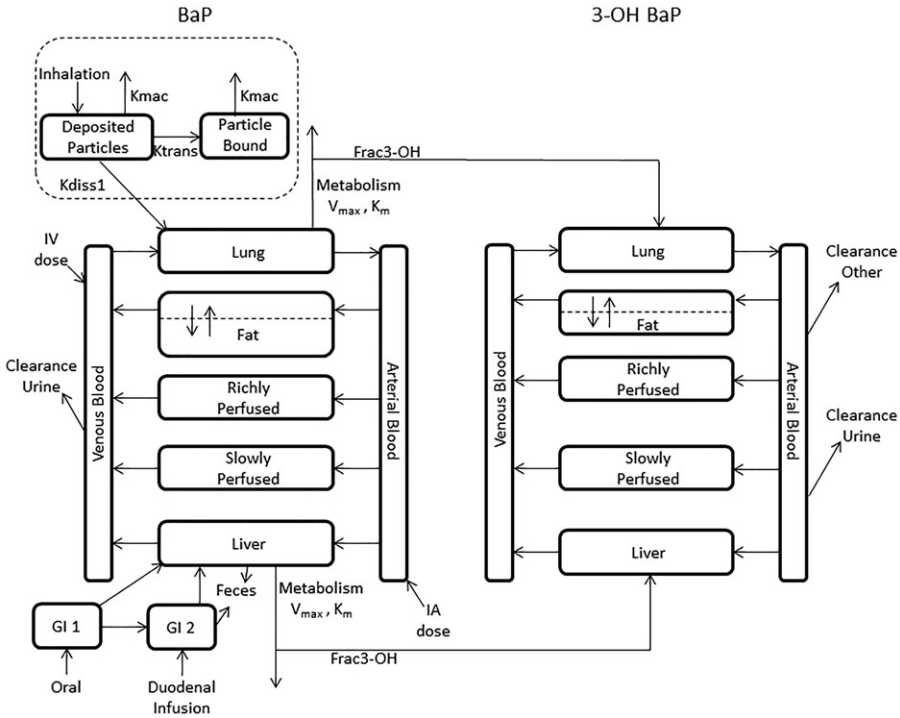

Figure 1. Diagram of the PBPK model for inhaled BaP. Dashed boxes denote structural enhancements added to the Crowell et al. (2011) PBPK model for oral BaP exposures in rats.

considered for dosimetry of inhaled gases or pure aerosols (Pankow, 2001).

For chemical risk assessment of inhaled compounds, an estimate of the target tissue doses resulting from plausible environmental exposure scenarios is often the recommended dose metric (USEPA, 2005). In many cases, results of human epidemiology or animal toxicity studies provide only external, ambient air concentration data to compare to observed adverse effects. These external doses may have uncertainties in target tissue dose that arise from extrapolating across exposure regimens or species. Regulatory guidance exists for the extrapolation of external inhalation concentrations using physiochemical properties and known differences in pulmonary tract anatomy in some risk assessments, but this guidance does not allow for precise calculations of target tissue doses (USEPA, 1994).

Physiologically based pharmacokinetic (PBPK) models are mathematical descriptions of key organ systems involved in the intake, distribution, metabolism and elimination of chemicals. Such models may be used to predict internal doses arising from a variety of exposure levels and durations that may differ substantially from exposures reported in epidemiological and toxicology datasets. A PBPK model mathematically represents the body's various organ systems (including blood) as a series of interconnected compartments, using known physiological blood flows and inhalation rates, tissue volumes, tissue-specific metabolic rates and elimination rates. A preliminary PBPK model for BaP was developed by Crowell et al. (2011), which simulates orally ingested BaP in rats. However, this model was not designed to simulate inhalation exposures and was parameterized and tested using only rat data.

In this study, we report the extension of the Crowell et al. (2011) PBPK model to describe the pharmacokinetics of particle-borne BaP following inhalation in humans and rats. The model was extended using available data in the published literature (Ewing et al., 2006; Sun et al., 1982, 1984). The critical parameters needed to capture the behavior of BaP particle inhalation, fractional lung deposition, particle dissociation, lung metabolism and lung tissue dosimetry are described, and the modified PBPK model structure is presented. The ability of the model to simulate published data of inhaled BaP in rats and humans is shown. The impact of various processes on BaP lung dosimetry, such as clearance of deposited BaP to the GI tract and background dietary BaP exposure (in humans), is also assessed. Finally, key data gaps, which must be addressed in order to further refine and improve the current model structure, have been identified.

Methods

PBPK model structure

The inhalation model for BaP in rats and humans is an extension of a previously published oral BaP model for rats (Crowell et al., 2011). In the Crowell et al. (2011) model, BaP amounts (nmoles) and concentrations (μM) were estimated for the lung, liver, fat and richly and slowly perfused tissues (Figure 1). Oral bolus, duodenal and intravenous (IV) infusion exposure routes were modeled. Oral exposures were represented as a two-compartment GI tract, and metabolism of BaP to total metabolites was modeled in the lung and liver. Fecal elimination of BaP was also included. BaP transfer from blood to tissues was assumed to be blood-flow limited except for the fat compartment, which was diffusion-limited. The current model expands the description from Crowell et al. (2011) to include a description for the 3-OH BaP metabolite in order to simulate the limited human data available. Physiological parameters and rate constants are given in Table 1 for BaP and the 3-OH BaP metabolite. Elimination of free 3-OH BaP from plasma is described as two separate

Table 1. Physiological and biochemical parameters for inhaled BaP PBPK model.

Parameters	Symbol	Units	Rat	Human	Source/Comments
Body weight	BW	grams	250	73 000	Default; study-specific values used when provided; human (ICRP, 2002)
Deposition fraction in lower respiratory tract	DEPFRACLOWER	–	0.09–0.23	0.198–0.72	Study-specific estimates (MPPD; Moldoveanu et al., 2008)
Deposition fraction in Upper Respiratory Tract (airways)	DEPFRACUPPER	–	0.0–0.075	0.0	
Vapor fraction	VAPFRAC	–	–	0.043	Lu & Zhu (2006)
BaP-particle dissociation rate constant	KDISS1	min^{-1}	0.003–0.0316	0.005	Optimized or visually fit for rat and human set to rat
Deposited particle to bound particle transition rate	KTRANS	min^{-1}	0.0–0.0045	0.0035	
Pulmonary ventilation	QPC	ml/min/gram	Study Specific	0.42	Brown et al., 1997; ICRP, 2001 (moderate to heavy work)
Cardiac output (ml/min)	QC	ml/min	0.67*QP[a]	0.67*QP	Brown et al., 1997
Fractional blood flows (% cardiac output)					
Fat blood	QFATC	–	0.07	0.07	Brown et al., 1997
Liver	QLIVC	–	0.183	0.23	Brown et al., 1997
Richly perfused tissues	QRICHC	–	0.4	0.4	Brown et al., 1997
Fractional tissue volumes (% body weight)					
Arterial blood	VARTC	–	0.025	0.025	Brown et al., 1997
Venous blood	VVENC	–	0.050	0.050	Brown et al., 1997
Fat	VFATC	–	0.065	0.214	Brown et al., 1997
Liver	VLIVC	–	0.037	0.026	Brown et al., 1997
Fat that is blood	VFATBLDC	–	–	0.02	Brown et al., 1997
Lung	VLNGC	–	0.005	0.008	Brown et al., 1997
Poorly perfused tissues	VPOORC	–	0.6	0.437	Brown et al., 1997
Macrophage particle clearance	K_{mac}	min^{-1}	0.000025	0.000025	MPPD ver 2.21
Absorption rate from theoretical stomach	KAS	min^{-1}	0.0005	0.0005	Visually fit to Moreau et al., 2015 oral data
Absorption rate from theoretical intestines	KAI	min^{-1}	0.0006	0.0006	Visually fit to Moreau et al., 2015 oral data
Gastric emptying rate	KSI	min^{-1}	0.0006	0.0006	Visually fit to Moreau et al., 2015 oral data
Fecal elimination rate	KIF	min^{-1}	0.0015	0.0015	Visually fit to Moreau et al., 2015 oral data
Diffusion rate constant for parent compound	PAFATPC	–	0.25	0.25	Optimized by Crowell et al., (2011) for Schlede et al., 1970
Diffusion rate constant for metabolite	PAFAT3C	–	0.25	0.25	
Tissue/blood partition coefficients (BaP)					
Fat	PFATP	–	436	436	Crowell et al., 2014
Liver	PLIVP	–	13.31	13.31	
Poorly perfused tissue	PPOORP	–	6.99	6.99	
Richly perfused tissue	PRICHP	–	13.31	13.31	
Lung	PLNGP	–	13.31	13.31	
Fraction of BaP bound in blood	FB	–	0.9	0.9	Optimized and fitted to Schlede et al., 1970

(*continued*)

Parameters	Symbol	Units	Rat	Human	Source/Comments
Tissue/blood partition coefficients (metabolite 1)					
Fat	PFAT3	–	401	401	Calculated Poulin & Krishnan, 1995; Poulin & Theil, 2000
Liver	PLIV3	–	12.24	12.24	
Poorly perfused tissue	PPOOR3	–	6.43	6.43	
Richly perfused tissue	PRICH3	–	12.24	12.24	
Lung	PLNG3	–	12.24	12.24	
Fraction of 3-OH BaP bound in blood	FB3	–	0.9	0.9	Set to BaP
Maximal rate of metabolism in liver	VMAXLIVPA	nmol/min/mg microsomal protein	1.08	0.025	Crowell et al., 2014; Barter et al., 2007
Maximal rate of metabolism in lung	VMAXLNGPA	nmol/min/mg microsomal protein	1.08	0.025	Liver value, adjusted for lung microsomal protein content from Wiersma & Roth, 1983
Michaelis constant for metabolism in liver	KMLIVPA	nmol/mL	17.97	0.725	Crowell et al., 2014
Michaelis constant for metabolism in lung	KMLNGPA	nmol/mL	17.97	0.725	Assumed identical to liver
Microsomal protein content per g liver	MMPPGL	mg/g	45	40	Houston & Galetin, 2008
Microsomal protein content per g lung	MPPGLNG	mg/g	3.67	2.27	Rietjens et al., 1988; Prough et al., 1977
Fraction BaP metabolized to 3-OH BaP	FRAC3	–	0.185	0.185	Heredia Oritz & Bouchard 2014
Urinary clearance 3-OH-BaP	CLURN3C	nmol/min/$BW^{0.75}$	0.0133	0.029	Set to approximate GFR; Chan et al., 1997; ICRP, 2001
Other clearance of 3-OH-BaP	CLOTH3C	ml/min/g Liver	0.4	1.92	Visually estimated

[a]QP = QPC × BW.

clearances with one representing urinary clearance and the other accounting for a lumped metabolic/fecal clearance to reduce the number of parameters to be estimated.

Crowell et al. (2011) calculated tissue/blood partition coefficients based on octanol/water partition coefficients (log *p*) and tissue composition (Poulin & Krishnan, 1995; Poulin & Theil, 2000), rather than deriving them experimentally, due to substantial binding of BaP to the apparatus used for measurement. The log *p* value used for BaP was 6.19, predicted by Advanced Chemistry Development (ACD) Labs (ACD Labs, 2015), which is similar to the published range of 5.99–6.04 (Mallon & Harrison, 1984). The partition coefficients for the 3-OH BaP metabolite were calculated using the same method as used by Crowell et al. (2011) for BaP. The ACD Labs log *p* for 3-OH BaP is 5.68 which is only slightly less lipophilic than that of BaP.

In vitro to *in vivo* extrapolation (IVIVE) was used to incorporate metabolism of BaP in the liver and lung. Metabolism of BaP was assessed in pooled rat and female human liver microsomes with maximum rate (V_{max}) and affinity (K_m) reported (Crowell et al., 2014). The affinity constant was used as reported; however, the V_{max} required scaling to the tissue. Scaling of the V_{max} was accomplished by multiplying the reported rate by the tissue-specific microsomal protein content per gram of tissue for liver or lung and then by the tissue volume. In this effort, the 3-OH BaP metabolite was used to compare to reported values from kinetic studies. The fraction of BaP metabolized to 3-OH was set as a fraction of the amount of total BaP metabolized in liver and lung using the value reported by Heredia-Ortiz et al. (2014).

In order to simulate inhalation exposures for the current assessment, the Crowell et al. (2011) model was implemented using the acslX simulation software (version 3.0.2.1, Egis Technologies, Huntsville, AL) and modified to simulate BaP-carrier particle inhalation. Modifications included adding parameters for inhalation exposure concentration and timing, alveolar ventilation and fractional deposition of inhaled particles in the upper (DepFracUpper) and lower (DepFracLower) respiratory tract. For this effort, DepFracUpper corresponds to all airways prior to the trachea and DepFracLower corresponds to all airways starting at the trachea. Consistent with most physiological parameters used by Crowell et al. (2011), alveolar ventilation rates were taken from Brown et al. (1997). Fractional deposition of BaP-carrier particles in the upper and lower respiratory tract was estimated using the multiple-path particle dosimetry (MPPD) model software package, as described below (Anjivel & Asgharian, 1995). Dissociation of deposited BaP from carrier particles was implemented by introducing a first-order rate constant by which BaP would be transferred to the lung tissues. Data were not available to define perfusion-limited BaP transport across the lung epithelium to the arterial blood (Pankow, 2001). Therefore, dissociated BaP was assumed to enter the total lung tissue volume, where it would be subject to saturable oxidative metabolism, based on the *in vitro* metabolic parameters of Crowell et al. (2014), scaled up to the liver and lung.

Deposited particle-associated BaP in the lung can be cleared via two processes in this model. The first is to be

Table 2. BaP-carrier particle characteristics and exposures for studies used in PBPK model parameterization.

Source	Species	Particle type (diameter, GSD[a])	Particle concentration (mg/m^3)	BaP concentration (mg/m^3)	Exposure duration	Fraction or mass of BaP deposited in Lung	Dose metric endpoints
Ewing et al., (2006)	SD Rat	Silica (3.5[b], 1.73)	680–3000	0.07–555	2 min	2.2–8400 μg	BaP in lung perfusate
Sun et al., (1982)	F-344 Rat	$^{67}Ga_2O_3$ (0.1[c], 1.6)	3.5	0.6	30 min	22.4%	Lung, liver, blood, GI tract radioactivity
Sun et al., (1984)	F-344 Rat	Diesel soot (0.13[c], 1.5)	3.9	0.006	30 min	16%	Lung, liver, blood, GI tract radioactivity
Lafontaine et al., (2004)	Humans	Not reported	Not Reported	0.00002–0.0015	4-10 h	19.8%[d]	Urinary 3-OH BaP

[a]Geometric standard deviation.
[b]MMAD: Mass median aerodynamic diameter (μm).
[c]MMD: Mean aerodynamic diameter (μm).
[d]Estimated with MPPD software ver. 2.11 using a particle size of 0.3 μm (MMAD) and GSD of 3.0 (treated as a polydisperse particle distribution by MPPD). All others were supplied in the published papers.

released into the lung-lining fluid and taken up by the lung as described earlier. The second is to remain adhered to the particles deposited in the lung and be cleared via the mucociliary escalator (rapid clearance) or engulfed by macrophages (slow clearance). The slow clearance process for [^{3}H]-BaP bound to carbon-based particles (i.e. diesel exhaust) dominates the total clearance of BaP deposited in the respiratory tract. The estimated first-order rate constant for slow particle clearance from the rat lung (K_{mac}) was set to be consistent with the slope of the terminal phase clearance of [^{3}H]-BaP reported in the Sun et al. (1984) study, where [^{3}H]-BaP was coated on diesel particles. For the Sun et al. (1984) study, it was apparent from the terminal-phase clearance that only a fraction of the BaP was bioavailable in the lung, with the rest remaining bound to and cleared with the diesel particle. In simulating the (Sun et al., 1982) gallium oxide ($^{67}Ga_2O_3$)-coated particles and (Ewing et al., 2006) silica-coated particles, it was assumed that all BaP was bioavailable and would be absorbed into the lung. With K_{mac} fixed to the rate of particle clearance, this limited the number of parameters that had to be estimated to describe the release of particle associated BaP to the rate of dissociation into the lung lining fluid (K_{diss1}), which was visually fit independently for all three studies and the rate of sequestration from absorption (K_{trans}), which was used only for the diesel particle simulation. The bioavailability of BaP determined for the rat was used to simulate human inhalation exposure scenarios under the assumption that bioavailability would be similar for all carbon-based particle-associated BaP.

Urinary elimination of free 3-OH BaP (CLURN3C) was described as a clearance process from the venous blood compartment and set to approximate the glomerular filtration rate (GFR) of the free fraction of 3-OH in plasma. The only human BaP-specific biomarker data available that included individual inhalation exposure information was for creatinine-corrected 3-OH-BaP concentration in urine of workers exposed to PAHs including BaP (Table 3) in occupational settings (Lafontaine et al., 2004). Age-, weight-, height-(assumed to be 30 years (yrs), 73 kg, and 176 cm, respectively, to represent a typical adult male worker; ICRP, 2002) and gender-dependent daily creatinine generation and excretion into the urine were modeled using the Cockcroft and Gault equation (Mage et al., 2004):

Table 3. Airborne BaP levels and associated maximum urinary 3-OH-BaP concentrations in occupationally-exposed workers (Lafontaine et al., 2004)[a].

Subject	Airborne BaP (mg/m^3)[b]	Measured urinary 3-OH-BaP (nmol/molCreat)	Simulated urinary 3-OH-BaP (nmol/molCreat)
1	2.41E-05	2.65E-01	1.02E-01
2	7.23E-05	2.25E-01	1.95E-01
3	9.65E-05	3.97E-01	2.41E-01
4	1.40E-04	3.18E-01	3.24E-01
5	1.40E-04	5.43E-01	3.24E-01
6	1.52E-04	6.23E-01	3.47E-01
7	2.10E-04	3.18E-01	4.58E-01
8	2.32E-04	3.84E-01	5.01E-01
9	3.01E-04	3.31E-01	6.33E-01
10	3.26E-04	5.03E-01	6.81E-01
11	4.24E-04	1.27E+00	8.68E-01
12	4.39E-04	1.46E+00	8.97E-01
13	5.18E-04	1.31E+00	1.05E+00
14	5.38E-04	1.91E+00	1.09E+00
15	7.07E-04	7.02E-01	1.41E+00
16	7.36E-04	1.66E+00	1.47E+00
17	1.50E-03	2.87E+00	2.93E+00

[a]Urinary clearance rate for 3-OH BaP was visually estimated to minimize the difference between measured and simulated urine concentrations and maintain a ratio of ±2 for all individuals with a mean of 1.0.
[b]The fraction deposited estimated using a MMAD of 0.3 μm and GSD of 3.0 (treated as a polydisperse particle by MPPD).

$$\text{Male } \mu\text{g creatinine/day} = 1.93 \times (140 - \text{age (yrs)}) \times \text{weight (kg)}^{1.5} \times \text{height (cm)}^{0.5}$$

$$\text{Female } \mu\text{g creatinine/day} = 1.64 \times (140 - \text{age (yrs)}) \times \text{weight (kg)}^{1.5} \times \text{height (cm)}^{0.5}$$

Daily creatinine-corrected urinary 3-OH-BaP excretion was thus calculated as the cumulative amount of 3-OH-BaP eliminated to the urine divided by the daily creatinine amount excreted. The Lafontaine data were used to estimate combined ''other'' clearance rate constant for free 3-OH-BaP (CLOTH3C) by fitting the model to the available human creatinine-adjusted urinary concentrations reported by Lafontaine et al. (2004).

In order to account for the presence of BaP in the human diet, a parameter for daily dietary intake was introduced to the model. Estimates of daily BaP ingestion in the United States and international diets vary widely (Buckley & Lioy, 1992; Chen et al., 2012; Deziel et al., 2011; EFSA, 2008). To characterize a potential population intake from diet, a median dietary BaP intake value estimated by the European Food Safety Authority (EFSA, 2008) (235 ng BaP/day) was used. Assuming an average body weight (BW) of 73 kg, the mean daily BaP dietary dose of 3.22×10^{-6} mg/kg/day (EFSA, 2008) was added to the model to account for the potential contribution from diet, with intake rate averaged over a 16-hour waking period (Shamoo et al., 1991).

Data used for model parameter estimation

A search of the published literature, using the PubMed bibliographic database to review study abstracts, was performed to identify studies containing data for the time course of inhaled BaP in the rat or human lungs, blood, or urine. Specifically, searches of the PubMed database were conducted to identify any published studies containing time course data following inhalation exposure to BaP-coated particles that would inform the rate of BaP dissociation from the particles and rate of appearance of BaP or total metabolites in the blood. Several studies were reviewed, but not used for model parameter estimation and evaluation because of the lack of time course granularity (Mitchell 1982, 1983; Ramesh et al., 2001; Withey et al., 1993; Wolff et al., 1989) or inconsistent results using identical experimental methods (Hood et al., 2000; Ramesh et al., 2002). Table 2 summarizes the relevant studies identified during the literature search for parameter estimation. These include one rat study of BaP-coated silica particles containing time course data useful for estimating BaP-particle dissociation (Ewing et al., 2006), two rat studies of different BaP-coated particle types ($^{67}Ga_2O_3$ and diesel soot) with time course data of total BaP radioactivity, which were used to test the rat model performance (Sun et al., 1982, 1984), and a rat study of oral and intravenous BaP exposure with BaP and 3-OH BaP plasma time course data (Moreau & Bouchard, 2015). One study of human workers containing data for the BaP-specific urinary biomarker, 3-OH BaP, associated with individual measurements of airborne BaP (Lafontaine et al., 2004) was also identified. A brief summary of these studies is provided below.

Rat studies

Ewing et al. (2006) reported the time course of BaP in isolated, ventilated and perfused (IVP) female Sprague-Dawley rat lungs. Uniform silica particles (680, 1300 and 3000 mg/m^3) were coated with BaP and introduced via a 2 s breath with a tidal volume of 1.9 ml/breath and a rate of 75 breaths/min for 2 min into the isolated trachea at three different BaP particle concentrations (0.065, 1.73 and 554.7 mg/m^3). Ewing et al. (2006) measured the deposition fraction in the lung for their system, which varied from 20% at the lowest concentration to 9% at the highest concentration. The reported deposition fraction in the article was retained for simulation in lieu of the MPPD model prediction because this allowed the simulation to maintain consistency with the reported data, and the tidal volume and breathing rate were controlled by the researcher. The initial deposition of BaP in the lung was 2.2 ± 0.4, 36 ± 4 and 8400 ± 900 ng for the low-, medium- and high-exposure group. BaP and pulmonary first-pass metabolites were collected in the system perfusate, as they diffused from the lung tissues to the underlying capillary bed. Ventilation rate was carefully controlled. The study authors reported concentrations of BaP appearing over approximately 70 min in the study system perfusate solution.

The studies of Sun et al. (1982, 1984) were used to evaluate the ability of the model to simulate the multiday (16–25 days) time course of BaP plus total metabolites in the lungs of rats inhaling BaP-coated particles of either $^{67}Ga_2O_3$ (Sun et al., 1982) or diesel exhaust particles (Sun et al., 1984). The study authors exposed (nose-only) male and female Fischer-344 rats to 0.6 mg/m^3 [^{3}H]-BaP coated on 3.5 mg/m^3 $^{67}Ga_2O_3$ particles for 30 min (Sun et al. 1982) with a reported mass deposited of 22.4% which was used directly in the simulation of this study with the BaP PBPK model. The study authors reported the lung clearance of deposited [^{3}H]-BaP as the reduction in the percent of initial deposited radiolabeled BaP equivalents (0.0049 mg), starting at the end of the inhalation period and continuing up to 16 days post exposure. The ^{3}H isotopic marker in the upper respiratory tract, GI tract, blood, liver and kidneys was measured in groups of four rats (2 male and 2 female) sacrificed at 2, 6 and 12 h and 1, 2, 5, 8 and 16 days postexposure. The measured radioactivity included an unknown combination of parent BaP, phase-I and phase-II metabolites and tissue adducts.

Sun et al. (1984) also reported the time course of radioactivity clearance from the lungs of male and female Fischer-344 rats following 30-minute inhalation (nose only) exposures of 0.0055 mg/m^3 [^{3}H]-BaP coated on 3.9 mg/m^3 denuded diesel soot particles. The study authors used an assumed particle fractional deposition of 16% and minute ventilation rate of 270 ml/min to calculate an initially deposited [^{3}H]-BaP dose of 7.1 ng. The initial deposition of BaP in the lung reported was used in the simulation of this study. As was done earlier by the same research group (Sun et al., 1982), lung clearance of deposited [^{3}H]-BaP was represented as the reduction in the percent of initial deposited radioactive BaP dose over time. Data for the ^{3}H radioactivity in the GI tract, blood, liver and kidneys, as well as cumulative radioactivity in the urine and feces, were measured in groups of four rats (2 male and 2 female) sacrificed at 30 min, 2, 6 and 12 h and 1, 2, 5, 8, 16, 20 and 26 days postexposure.

Moreau & Bouchard (2015) reported on the plasma time course of BaP and 3-OH BaP after administration of BaP to Sprague-Dawley rats. The administered dose was 40 µmol/kg administered as an intravenous or oral bolus. Plasma concentration was assessed at 1-, 2-, 4-, 8-, 12-, 24-, 48- and 72-h postdosing. Intratracheal and dermal routes were reported; however, these datasets are not included in this effort. The 3-OH BaP time-course data were used to visually estimate the CLOTH3C.

Human studies

No studies were identified in the published literature in which lung or blood levels of BaP were reported in humans following inhalation of measured levels of BaP. Thus, searches were conducted to identify literature on urinary biomarkers of PAH exposure to identify possible data for verifying the performance of the human model. Lafontaine et al. (2004) provided the only data for urinary metabolites levels associated with individual breathing zone measurements of BaP. Lafontaine reported the creatinine-adjusted 3-OH BaP concentrations in urine collected over 48 h from 16 workers exposed to PAHs while working two shifts at aluminum, creosote, carbon disk brake, electrometallurgy or shooting target production facilities. All workers had at least 36 h without occupational exposure prior to start of urine collection which began preshift on the first day of collection with urine collection continuing until the preshift sample collected the following day on the second day of exposure. The study authors reported the average creatinine-corrected urinary 3-OH BaP levels plotted against mean ambient air BaP levels measured as personal breathing zone samples collected during the two workdays (Table 2). Although there were no data for worker body weights, gender, smoking habits, or PAH and BaP particle size characteristics, these data were the only data identified correlating personal airborne exposure levels of BaP with an internal dose metric for humans. To simulate the Lafontaine study with the model, it was assumed that workers were exposed for 8 h/day and 5 days/week. Prior to calculating the average creatinine adjusted urinary concentration over the first two days after a 48-h period without exposure, the worker exposure was simulated for 15 weeks to allow stable periodicity to be reached in the simulated workers plasma and urine profiles (data not shown).

Parameter estimation

The fraction of BaP-carrier particles deposited in the respiratory tract of the rat and human (when not reported in the study) were calculated using the MPPD model software package (version 2.11), available freely online from Applied Research Associates (http://www.ara.com/products/mppd.htm). For the Sun et al. studies in rats (1982, 1984), study-specific values for particle mean aerodynamic diameter (MMAD), geometric standard deviation (GSD), and total aerosol concentration (Table 2), breathing frequency, body orientation (lying on stomach) and breathing scenario (nasal, oral, endotracheal) were used. For Ewing et al. (2006), the measured fraction deposited reported in the study was used in lieu of the MPPD model, as this was considered more accurate. Simulation of the occupational exposure to BaP described by Lafontaine et al. (2004) was employed to estimate the urinary clearance of BaP-hydroxylated metabolite. The particle size was assumed to be 0.3 μm mass median diameter (MMAD) and were assumed to have a GSD of 3.0, treated as a polydisperse particle by the MPPD software for fraction deposited determination, to reflect the particle size distribution reported in the IARC monograph for carbon black (IARC, 2010), and breathing was assumed to be oral nasal with tidal volumes of 625 ml for humans. For human simulations, default values in the MPPD software were used for particle density (1 g/cm^3), upper respiratory tract volume (50 ml) and the functional residual capacity of the lung (3300 ml). Regional fractions of the whole lung were calculated, with the lung depositional fraction (DepFracLower) defined as the sum of the tracheobronchial and deep pulmonary fractions which includes all airways below from the trachea (i.e. the zero generation). The fraction deposited in the upper respiratory tract (DepFracUpper) was also estimated by the MPPD model and includes all airways above the trachea. The MPPD model was only used to address the particle deposition in the two-compartment respiratory tract. The particle-associated BaP is treated as described earlier where BaP is dissociated from the particle and available for uptake in the lung or cleared from the lung still associated with the particle. To be conservative, all of the BaP cleared from the lung associated with particle is assumed transferred to the oral uptake model where all of the BaP is assumed released from the particle and available for oral absorption.

Optimization of K_{diss1} to the appearance of BaP in perfusate (Ewing et al., 2006) was carried out in acslX using the Nelder-Mead algorithm and with heteroscedasticity set to zero. Successful estimation of K_{diss1} was achieved for all three concentrations. The optimized value of K_{diss1} for the three exposure concentrations were 0.0316, 0.0119 and 0.0044 h^{-1} for the 0.065, 1.73 and 554.7 mg/m^3 exposures, respectively. K_{diss1} (0.003 h^{-1}) was visually estimated to provide the best fit to the loss of BaP from lung reported by Sun et al. (1982) after the optimization routine in acslX failed to converge. For the BaP-coated diesel particle study (Sun et al., 1984), both dissociation and uptake of BaP from the lung (K_{diss1}, 0.005 h^{-1}) and sequestration from particle release (K_{trans}, 0.0045 h^{-1}) were visually estimated to provide the best fit to the lung concentration time-course data after optimization failed to converge.

The human data for BaP-specific exposure and internal dosimetry only include creatinine-corrected urinary 3-OH BaP levels. Urinary clearance of 3-OH BaP was described as clearance from the plasma of free 3-OH BaP and was set to approximate GFR for rat and human. The proportion of BaP metabolized to 3-OH BaP was set to 0.185, which was reported by Heredia-Ortiz et al. (2014) and is similar to the 0.2 reported for rats in Ramesh et al. (2001) and to the conversion rate seen for pyrene (St. Charles et al., 2013). The rate of other clearance of 3-OH BaP (CLOTH3C) was described as clearance of free BaP from venous plasma. CLOTH3C represents all other clearances for 3-OH BaP for which there were no data available to parameterize the clearance of BaP in human. The rate constant was estimated visually for the rat to fit the IV and oral bolus time-course data in rat (Moreau & Bouchard, 2015) and the urinary excretion of 3-OH BaP in the occupational exposure study that compared BaP exposure to 3-OH BaP levels in workers of a carbon black disk production facility (Lafontaine et al., 2004). Simulations of human occupational inhalation exposures, assuming negligible dermal exposures, were run for 8 hours using airborne BaP levels reported by Lafontaine et al. (2004). A uniform, respirable particle size

was assumed (0.3 μm MMAD, with a GSD of 3.0 as reported by IARC, 2010 for carbon black occupational exposures). These values were entered into the MPPD model software, with all other MPPD parameters left as default values, resulting in a predicted DepFracUpper of 7% and DepFracLower of 19.8%. BaP in the gaseous phase was assumed to be 1% of the inhaled concentration. Particle-associated BaP is either available for uptake in the lung or cleared from the lung via a first-order process. Simulations of 8-hour inhalation exposures were run using selected personal air sampling BaP concentrations reported by the study authors (Table 3). The workers were simulated for 75 days of occupational exposure (8 h per day, 5 days per week) for 6 weeks and then the first 2 days after a 2 day rest were used to calculate the model predicted urine concentration over the 48 h. The urinary elimination rate constant (CLOTH3C) was adjusted until the simulated creatinine-corrected urinary 3-OH BaP levels were approximately within 2-fold of the urinary 3-OH BaP values reported by Lafontaine et al. (2004) for all subjects.

Impact of human dietary and rat secondary oral exposures on lung dosimetry

Two possible confounders that may affect the lung dosimetry of inhaled BaP are the fate of BaP depositing in the upper respiratory tract (URT; nose, nasopharynx, throat) and background BaP exposure in the human diet. Two exercises were conducted to examine the impact of these factors and to demonstrate the utility of the PBPK model for use in prioritizing data needs and future model refinement objectives. Simulations were conducted in the rat model following BaP inhalation (0.01, 0.1 and 1.0 mg/m^3 for 30 min) to determine the impact of secondary oral absorption of deposited BaP particles on two internal dose metrics: lung and venous blood BaP area under the concentration–time curve (AUC) (nmol × min/g tissue). For this exercise, it was assumed that 100% of the BaP deposited in the upper respiratory tract (DepFracUpper) was available for ingestion. The three BaP concentrations in the rat simulations spanned the range of BaP exposures reported by Ewing et al. (2006) and Sun et al. (1982, 1984). Additionally, simulation of a hypothetical smoking scenario in humans (20 and 40 cigarettes over 16 h per day) was used to assess the impact of dietary background BaP exposure on estimates of lung and blood BaP. Smoking conditions included two-second puff intervals, 30 s between puffs, puff volumes of 55 ml and 11 puffs/cigarette (Roemer et al., 2012). The rate constants K_{trans} and K_{diss1} were retained from the values estimated with the Sun et al. (1984) diesel particle lung concentration time course data. The mainstream smoke concentration was set to 0.027 mg/m^3, which results from the conservative assumption that all of the available BaP in the reference cigarette (approximately 16 ng) is inhaled during the 11 55 ml puffs. The exposure was divided into vapor (VapFrac) and particulate fractions (1-VapFrac), based on the reported fraction of BaP in cigarette smoke present in the vapor phase of 4.3% (Lu & Zhu, 2007). The total retention of BaP was set to 72% of the BaP inhaled (Moldoveanu et al., 2008). To be conservative, 100% of the vapor fraction was assumed to be taken up in the lung, and 100% of the retained particle mass of BaP was assumed deposited in the lower lung (i.e. DepFracLower). Of the mass of BaP associated with particles cleared from the lung, 100% of the bound BaP was assumed to be extracted from the ingested particle as there were no reported data to determine extraction of BaP from particle in intestinal fluid. Extracted BaP from particle was absorbed using the same oral absorption parameters as was used for the rat. Simulations were carried out for 75 days to allow the model to reach stable periodicity before assessing the maximum concentration of BaP in lung or plasma.

Sensitivity analysis

Analyses of the model output's sensitivity to the newly introduced model parameters were performed to determine which parameters are critical for continued model development and/or refinement. Sensitivity analyses were performed using the parameter estimation tool found in the AcslX software package (ver. 3.1.4.2) (Orlando, FL). The parameters of interest were varied by ±1% of their nominal values, and normalized sensitivity coefficients (the ratio changes in varied parameter to response variable, normalized to the nominal value of the varied parameter and the response variable) were calculated. The response variable was the lung tissue free BaP concentration taken at the end of the inhalation exposure interval for rats (30 min) or the end of a single cigarette exposure for human (5.1 min), using parameter values used to simulate the Sun et al. (1984) inhalation experiment for rats and generic smoking for humans. An inhalation exposure of 0.0055 mg/m^3 was used for rats based on the Sun et al. (1984) exposure and 0.027 mg/m^3 for cigarette smoke (Roemer et al., 2012). The normalized sensitivity coefficient reflects the fractional change in the model predicted dose metric (i.e. free BaP lung concentration) relative to the fractional change in the parameter value. Normalizing the coefficient to both the dose metric and the parameter value allows for the comparison of model constants between exposure scenarios and between model parameters.

Results

BaP rat simulations

From the study of Ewing et al. (2006), the optimization of K_{diss1} to each exposure provided good fits across the three exposure levels (Figure 2). The model-predicted perfusate concentration was well within a factor of 2 for nearly all time points and only deviated slightly from the shape of the data in the first 12 min of simulation for the highest exposure (554.7 mg/m^3). K_{diss1} was assumed to be dose-dependent as the time-course concentration in lung perfusate could not be fit with a single rate constant and was near linear when plotted against the natural log of exposure concentration ($r^2 = 0.84$; data not shown).

The time course data for percent of initial [^{3}H]-BaP equivalent radioactivity retained in the lung tissue (Sun et al., 1982) was predicted using the BaP PBPK model. The simulated percent of the initial amount deposited was

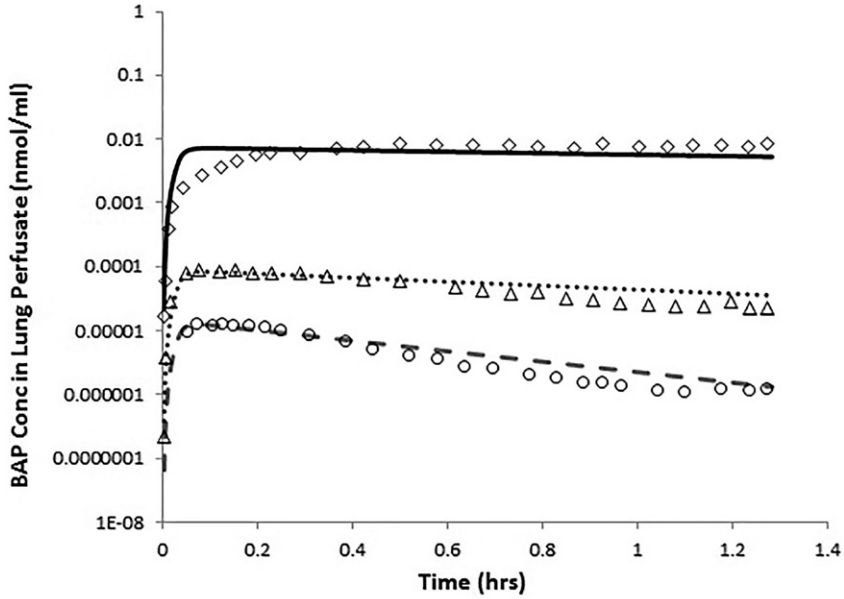

Figure 2. PBPK model predictions of BaP in the perfusate of SD rat lungs that are isolated, ventilated, and perfused (Ewing et al., 2006) following inhalation of BaP-coated silica particles (3.5 μm MMAD, 1.73 σ). Two-second puffs at 1.69 ml/breath, 75 breaths per minute were administered endotracheally at three concentrations (lines are for concentrations of 0.065 (dashed line, circles), 1.73 (dotted line, triangles) and 554.7 (solid lines, diamonds) mg BaP/m^3). Symbols indicate mean values of $n = 3$ rats.

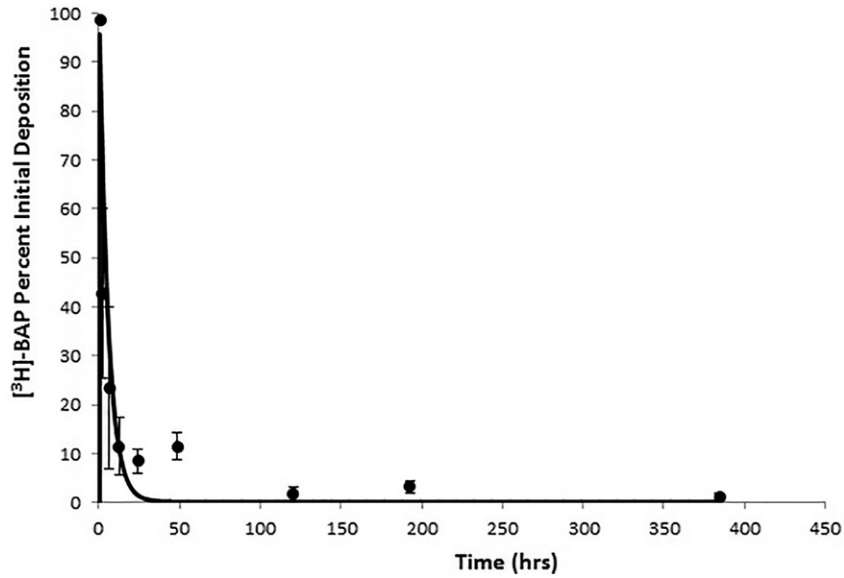

Figure 3. Model prediction of the percent BaP initially deposited from a single 30 min exposure to 0.6 mg/m^3 BaP (4.1 mg/m^3 total mass) coated on $^{67}Ga_2O_3$ particles. Data from Sun et al. (1982).

calculated as the accumulated mass deposited divided into the amount remaining at that time. Using the same assumptions as for Ewing et al. (2006) rat IVP data, the 30-min inhalation of 0.6 mg/m^3 BaP coated on $^{67}Ga_2O_3$ (3.5 mg/m^3) particles was used to estimate K_{diss1} to fit the lung time course reported by Sun et al. (1982) and is shown in Figure 3. While the model provides a good fit to the overall time course of percent initial deposition (i.e. within a factor of 3 of nearly all of the time points and consistent with the shape of the time-course curve), there was a sizable difference between the model and measured mass at 24 (6 fold lower) and 48 (55-fold lower) hours after exposure. As only the mean data were reported in Sun et al. (1982), we cannot assess whether this is within the experimental error of the study.

As was done for the Sun et al. (1982) data, the retained fraction of [^{3}H]-BaP equivalent radioactivity in the lungs was transformed to surrogate lung radioactive BaP- equivalent levels by multiplying the retained fraction at any time point by the study author-reported initial BaP dose (7.1 ng). Values for K_{diss1} and K_{trans} were estimated to provide the best fit to the lung time course data from a 30-min inhalation exposure to 0.0055 mg/m^3 BaP coated on 3.9 mg/m^3 diesel soot particles, as shown in Figure 4. Overall, the simulated time course of [^{3}H]-BaP radioactivity provides an excellent fit to the time course data for the mass of radioactivity remaining in lung with the simulations remaining well within a factor of 2 for all measured concentrations.

Simulation of the intravenous (top panel) and oral (bottom panel) administration of BaP to rat is shown in Figure 5 (Moreau & Bouchard, 2015). Incorporation of IVIVE to describe the metabolism of BaP provided good fit to the time-course percent of dose of both BaP and the metabolite, 3-OH BaP. For the parent, model-predicted plasma percent was within a factor of 3 for nearly all of the data with the exception of the first three time points collected after intravenous administration. For oral, the model was within a

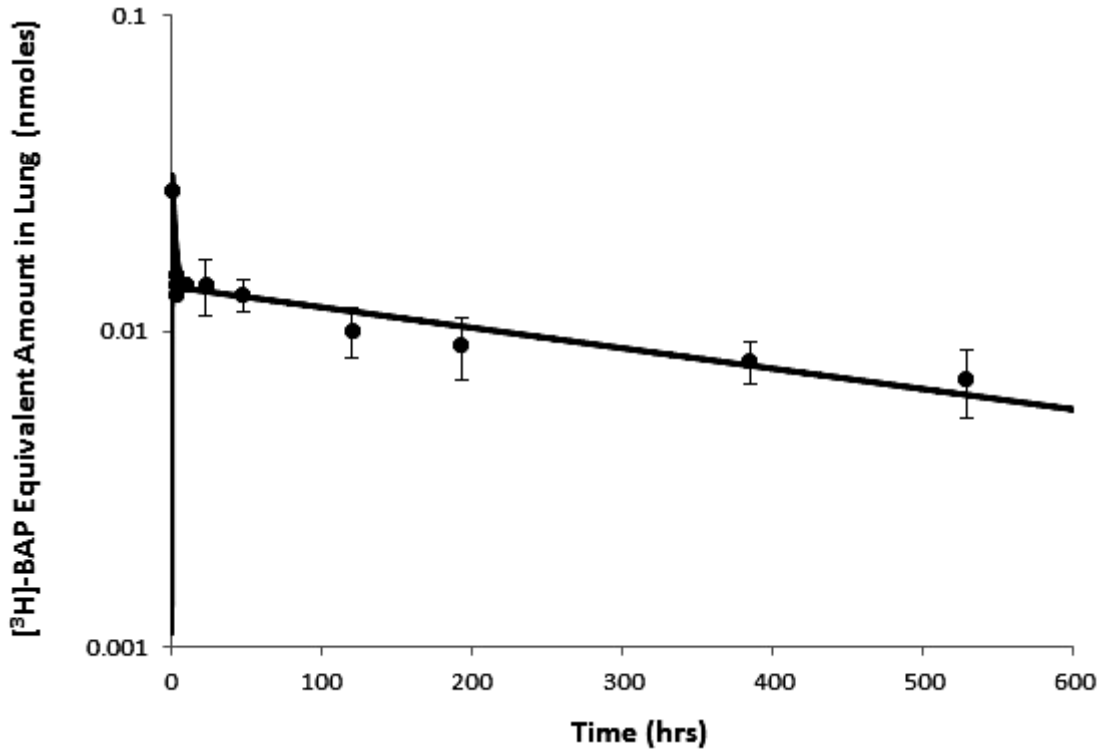

Figure 4. Model predicted amount of [3H]-BaP after a single nose-only exposure in rats to 0.0055 mg/m^3 [3H]-BaP (3.9 mg/m^3 total mass). Data from Sun et al. (1984).

factor of 3 for nearly all of the data with the 72-h sample within a factor of 3 of the reported value. For the 3-OH BaP metabolite, the model predicted percent was within a factor of 2 of nearly all of the measured values with the exception of 24-h time point for intravenous dosing.

BaP human simulations

The model-predicted pooled creatinine corrected urinary 3-OH BaP is compared with the measured concentrations in Table 3 (Lafontaine et al., 2004, 2006). The model prediction is within a factor of 2 for all subjects but one, which was within a factor of 3. It is worth noting that there is uncertainty in this predication as the particle size distribution employed in the simulation was for unrelated production facilities and CLOTH3C rate constant was estimated to provide the best fit to the data under the exposure conditions described earlier. Even with this uncertainty, the BaP model captures the relationship between exposure and urinary excretion of metabolite across a wide range of measured breathing zone concentrations.

Impact of simulated swallowing of URT-deposited BaP

The MPPD model predictions of regional lung deposition of BaP-carrier particles provided estimates of fractions of inhaled doses deposited in the head (or URT: nares, nasopharynx, throat), tracheobronchial region and deep alveolar spaces. However, the PBPK model particle dissociation parameter optimization did not take into account possible contribution of URT-deposited and swallowed BaP on lung or blood BaP dosimetry, primarily because the Ewing et al. (2006) IVP lung data provided an opportunity to parameterize BaP-particle dissociation in the isolation of mucociliary clearance or URT deposition and absorption. The impact of possible GI absorption of URT-deposited BaP was explored by simulating three different BaP inhalation levels (0.01, 0.1 and 1.0 mg/m^3) under the conditions of the Sun et al. (1982) experiment, and either including the URT-deposited fraction as a GI absorbed dose or excluding it altogether. These comparisons provide simplistic assessments of possible systemic BaP absorption from some combination of swallowed BaP that was initially deposited in the URT or rapidly cleared from the lung by mucociliary escalation. It was assumed that 100% of the URT-deposited BaP was dissociated from the carrier particle and available for GI absorption.

Table 4 shows the impact of including or excluding orally absorbed URT-deposited BaP on the lung and venous blood BaP AUCs (nmole $\times$ min/mg) from short-term exposures. Adding all of the URT-deposited BaP as a GI dose resulted in less than a 1% difference in these dose metrics for simulated inhalation exposures spanning three orders of magnitude. Thus, the exclusion of URT-deposited BaP from the simulation, at least for the dissociation rates and species tested, does not appear to significantly impact lung or plasma dosimetry for BaP when evaluated with these exposure conditions.

Impact of simulated dietary background BaP

The contribution of human dietary BaP exposures on blood BaP levels or lung BaP burden, via pulmonary tissue uptake from the systemic circulation, is unknown. This was explored by comparing a simulated hypothetical cigarette smoking regimen to a steady-state intake via dietary exposure using a

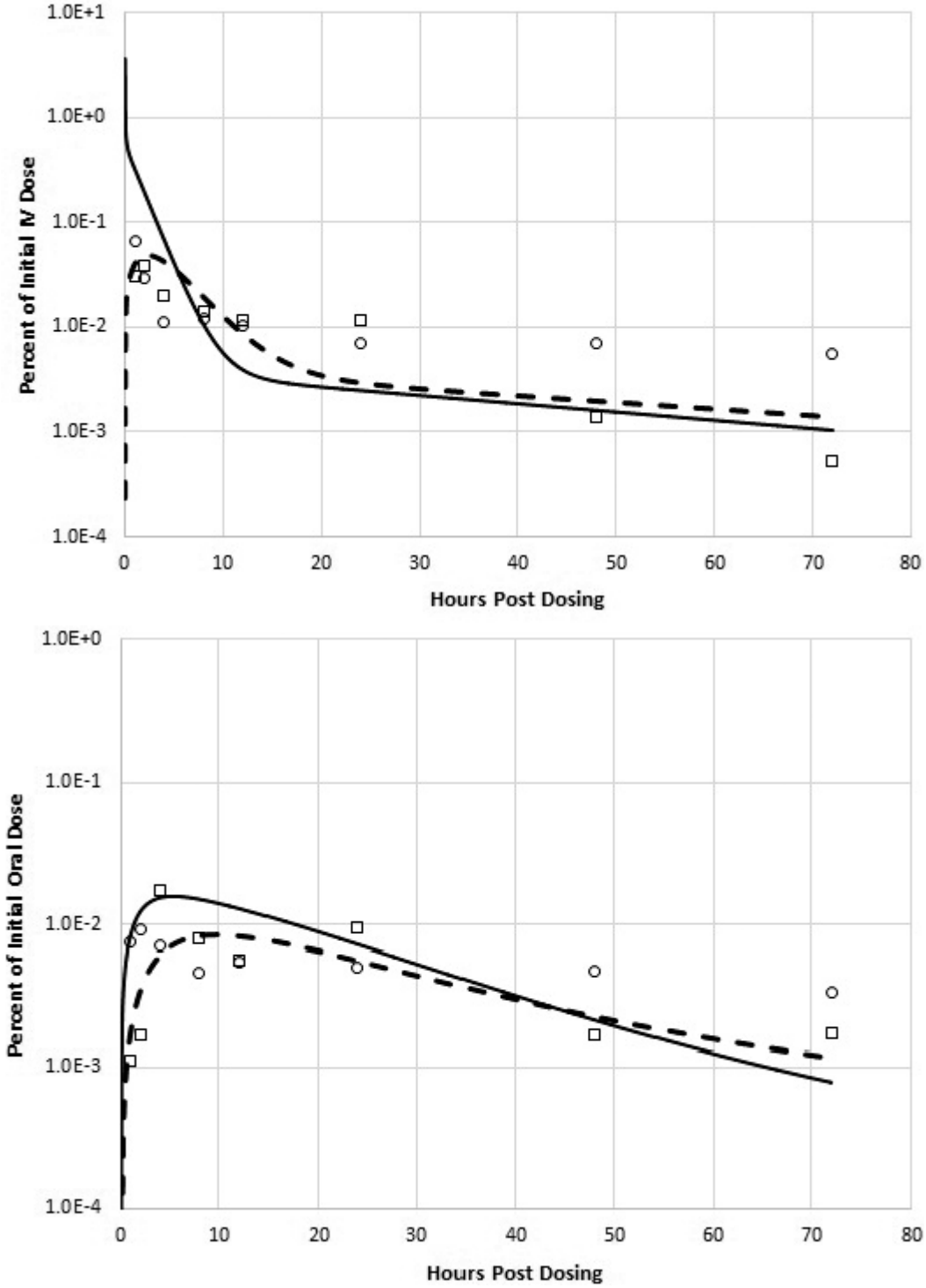

Figure 5. BaP model prediction of intravenous (top) and oral (bottom) time-course data for BaP (solid line, circles) and 3-OH BaP (dashed line, boxes) after a single bolus dose of 40 μmol/kg to male Sprague-Dawley rats. Data from Moreau and Bouchard (2015).

daily dose of 3.36×10^{-6} mg/kg/day (EFSA, 2008). Smoking of 20 or 40 cigarettes during a single day was simulated, using conditions reported by Roemer et al. (2012) for a reference cigarette and a hypothetical mainstream smoke BaP concentration of 0.027 mg/m^3 with 4.3% of the exposure represented as vapor (100% uptake into lung tissue, i.e. no buccal cavity extraction) and 72% of BaP mass retained as bound to particulate deposited in the lung compartment (Moldoveanu et al., 2008). The peak BaP concentration in lung and plasma compartments was assessed on the 75th simulated day to allow the model to reach stable periodicity (Table 5). The peak concentration in lung over the course of a day for smoking alone was 9.13×10^{-10} mg/g (1 pack per day) or 1.76×10^{-9} mg/g (2 packs per day), while the peak concentration in blood was 6.06×10^{-10} mg/ml for a pack per day smoker and 1.19×10^{-9} mg/ml for a 2 pack per day smoker. The time-weighted average lung and blood concentration from dietary intake alone was approximately 60% for lung and 66% for blood compared to a single pack per day usage. For a 2 pack/day smoker, the time-weighted average BaP

Table 4. Impact of considering mucociliary transport to the GI tract of BaP-containing particles deposited in the upper respiratory tract.

	Dose metrics			
	Ignoring GI transport of BaP deposited in upper respiratory tract		Assuming GI transport of BaP deposited in upper respiratory tract	
Exposurea (mg/m^3)	Lung BaP AUC (mg × min/g)	Venous blood BaP AUC (mg × min/ml)	Lung BaPAUC (mg × min/g)	Venous Blood BaP AUC (mg × min/ml)
0.01	0.0000233	0.0000166	0.0000235	0.0000167
0.1	0.000233	0.000166	0.000235	0.000167
1.0	0.00233	0.00166	0.00235	0.00167

[a]30-min nose-only exposures, per Sun et al. (1982).

Table 5. Comparison of the lung and venous blood maximum concentration after steady-state conditions were reached from either smoking 20 or 40 cigarettes per day, dietary exposure alone or to a combination exposure of 20 or 40 cigarettes per day and dietary exposure using the human BaP PBPK model assuming 100% bioavailability of ingested particles cleared via the mucociliary escalator (75 days of exposure were simulated to ensure stable periodicity with daily maximum concentration).

Cigarettes/Day	Scenario	Lung (mg/g)	Blood (mg/ml)
20 (1 pack)	Smoking alone	9.13E-10	6.06E-10
	Diet alone	5.35E-10	4.03E-10
	Smoking with diet	1.44E-09	1.00E-09
40 (2 packs)	Smoking alone	1.76E-09	1.19E-09
	Diet alone	5.35E-10	4.03E-10
	Smoking with diet	2.29E-09	1.59E-09

concentration from dietary exposure was approximately 30% of the predicted smoking associated maximum BaP concentration in lung and approximately 34% blood. Combined dietary and smoking exposure resulted in predicted peak lung and blood concentrations of 1.44 10^{-9} mg/g and 1.00×10^{-9} mg/ml for a pack/day smoker and 2.29×10^{-9} mg/g and 1.59×10^{-9} mg/ml for a 2 pack/day smoker. Interestingly, Lafontaine et al. (2006) reported 3-OH BaP in urine of smokers and nonsmokers who were not occupationally exposed to BaP. The median percent of 3-OH BaP in urine of nonsmokers compared to smokers was approximately 51% which is similar to the 48% predicted by the current model for a 1½ pack per day smoker (midpoint of use rates reported in the study as a range of 13 to 50) after simulation was allowed to reach stable periodicity.

Sensitivity analysis

The normalized sensitivity coefficients (i.e. the fractional change in a model output resulting from a fractional change in a model parameter) at the end of a 30-min exposure (rat) and last puff of a cigarette (human) are shown in Figure 6. Similar results are seen with both species/scenarios. The most sensitive parameters[1] for concentration in lung were the fraction bound in blood (FB), pulmonary ventilation rate (QPC) or rate of puff inhaled (QPuff), lung/blood partition coefficient (PLNGP) and the fraction of exposure that is vapor (VapFrac). Parameters with intermediate sensitivity were the BaP dissociation constant (K_{diss1}), deposition fraction (DepFracLower), and fractional volume of tissues including lung (VLNGC), venous blood (VVENC) or fat (VFATC) and poorly perfused tissue (VPOORC). Overall, the parameters with the most impact on lung concentration of BaP are those that are either well defined for rat and human (QPC, VLNGC, VFATC, VPOORC, DepFracLower) or have been determined experimentally for BaP (PLNGP, K_{diss1}, FB).

[1]Defined as those parameters with a normalized sensitivity coefficient of 10% or greater absolute value.

Discussion

A PBPK model for BaP in rats (Crowell et al., 2011) has been extended to include inhalation exposures of carrier particle-borne BaP in rats and humans. PBPK (Roth & Vinegar, 1990) and empirical biokinetic (Heredia-Ortiz et al., 2014) models for BaP have also been published, but neither included a description to account for the inhalation of aerosol particles which accounts for most of the inhaled BaP from occupational exposure or cigarette smoke. Chiang and Liao (2006) published a human inhalation PBPK model for BaP that was used to estimate health risks from incense smoke inhalation at temples in Taiwan. The Chiang model did not account for BaP deposition in the lungs as an aerosol/particle, nor did it provide specific rates of BaP dissociation from particulate solids. Chiang and Liao (2006) did not include any calibration of the model to human data nor did they demonstrate validity of the model performance (i.e. model simulation compared to human data). The work presented herein represents the first steps to develop a PBPK model of inhaled carrier particle-borne BaP in rats and humans and provides an example of the utility of iterative model development as a tool to inform parallel development of human and laboratory animal data needed to eventually develop a robust predictive computational tool suitable for use in risk assessment of inhaled BaP.

The focus of the present work was to add the capability of inhaled BaP lung tissue dosimetry to the oral BaP model of Crowell et al. (2011). BaP inhalation from occupational sources and tobacco smoking involves deposition of BaP-coated carrier particles throughout the respiratory tract (Miguel & Friedlander, 1978; Pankow, 2001). Thus, BaP inhalation dosimetry requires knowledge of the deposition pattern of BaP-laden particles in the respiratory tract and

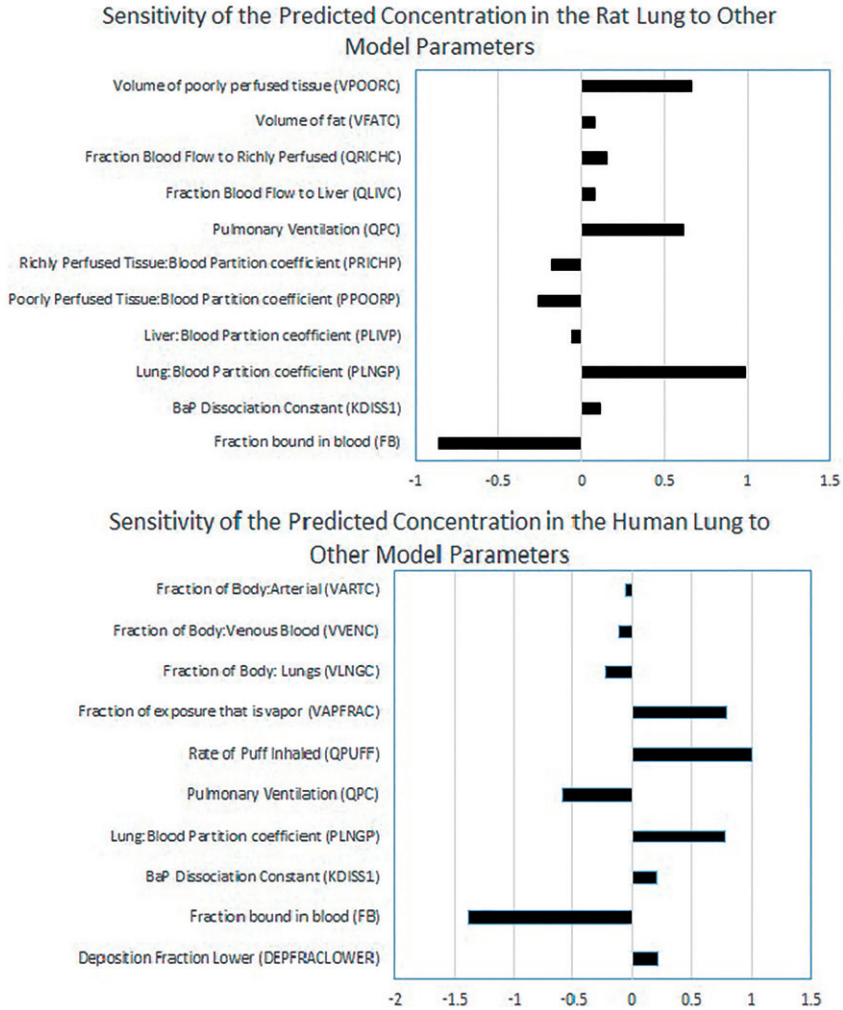

Figure 6. Normalized sensitivity coefficients for rat (top) and human (bottom) at end of exposure to 30-min inhalation of diesel exhaust particles (rat) or a single cigarette (human). These values show the relative effect of changes in these parameters on the value of the concentration in the lung (e.g. as the fraction bound in blood increases the concentration in the lung decreases but more for humans than rats).

BaP-particle dissociation characteristics in the respiratory mucus layer. The level of detail for particle physical characteristics and inhalation patterns can have a significant impact on predictions of BaP-particle lung deposition. In the present study, specific data reported in the assessment of the particle size distribution or deposition of particle-bound BaP or the predicted deposition of particles based upon the MPPD model were used to predict lung deposition and BaP kinetics given study-specific exposure parameters.

Once deposited in the airways and pulmonary region of the lung, BaP-carrier particles are immediately subject to clearance from the respiratory tract via mucociliary escalation and slow clearance by macrophage engulfment and subsequent sequestration to the lymph nodes (Gerde et al., 2001). The rate at which BaP dissociates from the carrier particle, and is then separated from the particle clearance mechanisms, is determined by the relative binding affinity of BaP to the particular particle type, coupled with the ability of the mucus to impart solvent desorption of the coated BaP (Gerde et al., 2001; Sun et al., 1984). The clearance of BaP particles in dogs and rats has been described as having bi-phasic time courses both short (<1 h) or days after deposition (Ewing et al., 2006; Gerde et al., 1993, 2001; Sun et al., 1982, 1984). It is not clear whether the bi-phasic clearance of BaP, and in some cases, its radiolabeled equivalents, is dependent on mechanical clearance, phagocytosis, macromolecular adduction or a combination of all three. In this effort, the uptake was dependent on source material of the particle used as the vehicle. $^{67}Ga_2O_3$ particle data were fit with a single rate constant for dissociation and uptake into lung tissue, while the terminal clearance of BaP with diesel particles more closely matched the rate of mucociliary clearance, with a fraction of the BaP inhaled being taken up into the lung tissue. The mass of particle-associated BaP may also play a role in bioavailability as reported by Ewing et al. (2006). The estimation of K_{diss1} for each exposure level was undertaken assuming that the dissolution from the particle is potentially saturable at the particle mucous interface as opposed to the cell diffusion limitation based upon octanol extraction of BaP from the particle proposed by Ewing et al. (2006). The dissolution-limited assumption or the tissue diffusion-limited assumption would provide the same result as the reported data (i.e. the uptake of BaP from particle is concentration dependent); however, given the consistency of the first-order dissolution description with the low concentration reported by Ewing et al., (2006), which was more relevant to human exposure levels simulated in this study, the use of a simple dissolution description is warranted.

Free BaP is available for luminal-to-apical diffusion through the lung tissue layers, where it is subject to initial

Table 6. Prioritized data needs for further refinement of a PBPK model for inhaled BaP.

Data need	Use for model refinement
In vitro	
1. Lung tissue metabolism parameters for BaP and downstream metabolites	Estimate human and rat lung V_{max}, K_m and glutathione conjugation values for BaP and phenol, diol and tetraol (and conjugate products) metabolites
2. Dissociation rate calculations in surrogate mucus layer solutions.	Estimate differences in early-phase BaP-particle dissociation for specific carrier particle types
3. IVIVE extrapolation of rat data from 2 and 3 to human lung	Estimate human values for lung and liver V_{max}, K_m and glutathione conjugation rates
Rat in vivo	
1. Rat time course data (>24 h) for BaP in lung and blood following exposure to BaP on multiple carrier particles	Validate estimates of carrier particle-specific BaP-particle dissociation rates
2. Rat time course data (>24 hs) for BaP in lung and blood following inhalation exposure to multiple BaP exposure levels.	Validate lung metabolism parameters for BaP and downstream metabolites
3. Respiratory tract region-specific dissociation and absorption rates	Delineate effect on region-specific lung dosimetry
4. Concurrent plasma and urine metabolite Profiles	Estimate renal elimination rates for multiple BaP urinary biomarkers
Human in vivo	
1. Studies of human populations that contain blood time course data for BaP and metabolites following well-characterized inhalation exposures.	Validate estimates of BaP-particle dissociation rates, lung V_{max} and Km values
2. Concurrent plasma and urine metabolite Profiles	Estimate renal elimination rates for multiple BaP urinary biomarkers, tissue-specific metabolic parameters, and effect of estimates of dietary background BaP

epoxidation and hydroxylation, followed by further glutathione conjugation and elimination to the blood, bile, urine and feces (Moir et al., 1998; Xue & Warshawsky, 2005). In extending the Crowell BaP model to include inhalation as a route of exposure, the distribution of absorbed BaP was not modified from the original model other than the addition of respiratory tract to allow description of particle-associated BaP, inclusion of species-specific lung BaP metabolism (V_{max} and K_m) using IVIVE and a simplistic description of 3-OH-BaP clearance in humans. Although the extended inhalation PBPK model could be refined to discriminate between deposition, dissociation and absorption of BaP into separate tracheobronchial and alveolar compartments, the available data do not support the derivation of separate clearance, metabolic and tissue diffusion parameters for these compartments as the metabolic constants were derived from total lung microsomes. The radiolabeled studies of Sun et al. (1982, 1984) do provide time course data for BaP-metabolite equivalents in various segments of the URT and airways, but the lack of metabolite predictive capability of the current model does not allow for that data to be utilized. Region-specific respiratory tract dosimetry of inhaled BaP and metabolites will be useful for future PBPK model refinement to further reduce uncertainty in model predictions.

The initial development of an inhalation BaP PBPK model has resulted in a model capable of predicting whole lung dosimetry and bioavailability of BaP in rats and humans following acute and chronic exposures to a combination of vapor and aerosol particulate of BaP and has served to distinctly clarify data need to proceed with development of a more robust model adequate for use in inhaled BaP risk assessment. Estimation and addition of pulmonary metabolism parameters for phase-I and pahse-II metabolites, adding diffusion-limited lung tissue transfer (if required) and determining particle-specific dissociation rate constants, all in the context of the lung airway and deep alveolar tissues, are steps that would enhance the current extended model. Table 6 lists prioritized data needs that, if filled, would allow for significant model advancement. *In vitro* evaluations of metabolite pharmacokinetics and dissociation rate constants in rodent and human lung cell and/or enzyme systems could be used for extrapolation to *in vivo* predictions using the approach that was successfully applied for BaP in this effort. Filling these data gaps could allow for greater use of the current radiolabeled time course data. Subsequent generation of *in vivo* plasma and/or urinary BaP and metabolite profile data in humans following carefully measured BaP-carrier particle exposures (such as tobacco smoking or occupational exposures) can then be used to iteratively verify and refine model parameters.

In conclusion, a preliminary inhalation BaP PBPK model structure is presented as an extension of the model developed by Crowell et al. (2011) that is capable of predicting lung dosimetry of BaP in rats and humans. The dearth of detailed data for BaP-only exposures in humans and BaP and specific metabolite time-course profiles in human and rodent blood and urine suggest the need for additional experimental data to further refine the model for making predictions of BaP and metabolite dosimetry from chronic exposures, as well as using existing and future human BaP biomarker data. However, the current modeling results from the application of the extended model are also illustrative of the application of PBPK models for use in experimental hypothesis testing. The results presented provide direction for experimentation to fill data gaps that would result in a refinement of a PBPK model for inhaled BaP that could be used in a variety of risk assessment contexts.

Declaration of interest

The authors with the exception of Dr. Crowell are either current/former employees of British American Tobacco or RJ Reynolds Tobacco Company or are contractors to the aforementioned companies. All work was funded by British American Tobacco (Investments) Ltd and RJ Reynolds Tobacco Company. The Authors declare that no financial or personal conflicts of interest exist with regard to the submission of this manuscript.

References

ACD Labs. (2015). Advanced Chemistry Development Labs. [Online] Available from: http://www.acdlabs.com/.

Anjivel A, Asgharian B. (1995). A multiple-path model of particle deposition in the rat lung. Fund Appl Toxicol 28:41–50.

Barter ZE, Bayliss MK, Beaune PH, et al. (2007). Scaling factors for the extrapolation of in vivo metabolic drug clearance from in vitro data: reaching a consensus on values of human microsomal protein and hepatocellularity per gram of liver. Curr Drug Metab 8:33–45.

Brown RP, Delp MD, Lindstedt SL, et al. (1997). Physiological parameter values for physiologically based pharmacokinetic models. Toxicol Ind Health 13:407–84.

Buckley TJ, Lioy PJ. (1992). An examination of the time course from human dietary exposure to polycyclic aromatic hydrocarbons to urinary elimination of 1-hydroxypyrene. Br J Ind Med 49: 113–24.

Chan BSH, Seale JP, Duggin GG. (1997). The mechanism of excretion of paraquat in rats. Toxicol Lett 90:1–9.

Chen YH, Xia EQ, Xu XR, et al. (2012). Evaluation of benzo[a]pyrene in food from China by high-performance liquid chromatography-fluorescence detection. Int J Environ Res Public Health 9:4159–69.

Chiang KC, Liao CM. (2006). Heavy incense burning in temples promotes exposure risk from airborne PMs and carcinogenic PAHs. Sci Total Environ 372:64–75.

Crowell SR, Amin SG, Anderson KA, et al. (2011). Preliminary physiologically based pharmacokinetic models for benzo[a]pyrene and dibenzo[def, p]chrysene in rodents. Toxicol Appl Pharmacol 257: 365–76.

Crowell SR, Hanson-Drury S, Williams DE, Corley RA. (2014). In vitro metabolism of benzo[a]pyrene and dibenzo[def, p]chrysene in rodent and human hepatic microsomes. Toxicol Lett 228:48–55.

Deziel NC, Strickland PT, Platz EA, et al. (2011). Comparison of standard methods for assessing dietary intake of benzo[a]pyrene. Cancer Epidemiol Biomarkers Prev 20:962–70.

EFSA (2008). European Food Safety Authority. Scientific opinion of the panel on contaminants in the food chain. EFSA J 724:1–114.

Ewing P, Blomgren B, Ryrfeldt A, Gerde P. (2006). Increasing exposure levels cause an abrupt change in the absorption and metabolism of acutely inhaled benzo(a)pyrene in the isolated, ventilated, and perfused lung of the rat. Toxicol Sci 91:332–40.

Gerde P, Muggenburg BA, Henderson RF. (1993). Disposition of polycyclic aromatic hydrocarbons in the respiratory tract of the Beagle dog III. Mechanisms of the dosimetry. Toxicol Appl Pharmacol 121: 328–34.

Gerde P, Muggenburg BA, Lundborg M, et al. (2001). Respiratory epithelial penetration and clearance of particle-borne benzo[a]pyrene. Resp Res Health Effects Inst 101:1–40.

Heredia-Ortiz R, Maître A, Barbeau D, et al. (2014). Use of physiologically-based pharmacokinetic modeling to simulate the profiles of 3-hydroxybenzo(a)pyrene in workers exposed to polycyclic aromatic hydrocarbons. PLoS One 9:e102570

Hood DB, Nayyar T, Ramesh A, et al. (2000). Modulation in the developmental expression profile of sp1 subsequent to transplacental exposure of fetal rats to desorbed benzo[a]pyrene following maternal inhalation. Inhal Toxicol 12:511–35.

Houston JB, Galetin A. (2008). Methods for predicting in vivo pharmacokinetics using data from in vitro assays. Curr Drug Metab 9:940–51.

IARC. 2010. IARC monographs on the evaluation of carcinogenic risks to humans, Volume 93, carbon black, Titanium Dioxide, and Talk. Lyon, France.

ICRP (The International Commission on Radiological Protection). (2001). Basic anatomical and physiological data for use in radiological protection: reference values. Valentine J (ed). ICRP Publication 89, Oxford, UK: Pergamon Press.

ICRP. (2002). Basic anatomical and physiological data for use in radiological protection reference values. ICRP Publication 89. Ann. ICRP 32 (3–4).

Lafontaine M, Gendre C, Delsaut P, Simon P. (2004). Urinary 3-hydroxybenzo[a]pyrene as a biomarker of exposure to polycyclic aromatic hydrocarbons: an approach for determining a biological limit value. Polycycl Aromat Comp 24:441–50.

Lafontaine M, Champmartin C, Simon P, et al. (2006). 3-Hydroxybenzo[a]pyrene in the urine of smokers and non-smokers. Toxicol Lett 162:181–5.

Lu H, Zhu L. (2007). Pollution patterns of polycyclic aromatic hydrocarbons in tobacco smoke. J. Hazard. Mater 139:193–8.

Mage DT, Allen RH, Gondy G, et al. (2004). Estimating pesticide dose from urinary pesticides concentration data by creatinine correction in the third national health and nutrition examination survey (NHANES-III). J Expo Anal Env Epidemiol 14:457–65.

Mallon BJ, Harrison FL. (1984). Octanol-water partition coefficient of benzo(a)pyrene: Measurement, calculation, and environmental implications. Bull Environ Contam Toxicol 32:316–23.

Miguel AH, Friedlander SK. (1978). Distribution of benzo[a]pyrene and coronene with respect to particle size in Pasadena aerosols in the submicron range. Atmos Environ 12:2407–13.

Mitchell C. (1982). Distribution and retention of benzo(A)pyrene in rats after inhalation. Toxicol Lett 11:35–42.

Mitchell C. (1983). The metabolic fate of benzo[a]pyrene in rats after inhalation. Toxicology 28:65–73.

Moir D, Viau A, Chu I, et al. (1998). Pharmacokinetics of benzo[a] pyrene in the rat. J Toxicol Environ Health Part A 53:507–30.

Moldoveanu SC, Coleman III W, Wilkins JM. (2008). Determination of polycyclic aromatic hydrocarbons in exhaled cigarette smoke. Beitr Tabakforsch Int 23:85–97.

Moreau M, Bouchard M. (2015). Comparison of the kinetics of various biomarkers of benzo[a]pyrene exposure following different routes of entry in rats. J Appl Toxicol 35:781–90.

Pankow J. (2001). A consideration of the role of gas/particle partitioning in the deposition of nicotine and other tobacco smoke compounds in the respiratory tract. Chem Res Toxicol 14:165–1481.

Poulin P, Krishnan K. (1995). An algorithm for predicting tissue: blood partition coefficients of organic chemicals from n-octanol: water partition coefficient data. J Toxicol Environ Health 46:117–29.

Poulin P, Theil FP. (2000). A priori prediction of tissue:plasma partition coefficients of drugs to facilitate the use of physiologically-based pharmacokinetic models in drug discovery. J Pharm Sci 89:16–35.

Prough RA, Sipal Z, Jakobsson SW. (1977). Metabolism of benzo(a)pyrene by human lung microsomal fractions. Life Sci 21:1629–35.

Ramesh A, Greenwood M, Inyang F, Hood DB. (2001). Toxicokinetics of inhaled benzo[a]pyrene: plasma and lung bioavailability. Inhal Toxicol 13:533–55.

Ramesh A, Hood DB, Inyang F, et al. (2002). Comparative metabolism, bioavailability, and toxicokinetics of benzo[a]pyrene in rats after acute oral, inhalation, and intravenous administration. Polycycl Aromat Comp 22:969–80.

Rietjens IM, Dormans JA, Rombout PJ, van Bree L. (1988). Qualitative and quantitative changes in cytochrome P-450-dependent xenobiotic metabolism in pulmonary microsomes and isolated Clara cell populations derived from ozone-exposed rats. J Toxicol Environ Health 24:515–31.

Roemer E, Schramke H, Weiler H, et al. (2012). Mainstream smoke chemistry and in vitro and in vivo toxicity of the reference cigarettes 3R4F and 2R4F. Beitr Tabkforsch 25:316–35.

Roth RA, Vinegar A. (1990). Action by the lungs on circulating xenobiotic agents, with a case study of physiologically based pharmacokinetic modeling of benzo[a]pyrene disposition. Pharmacol Therapeut 48:143–55.

Schlede E, Kuntzman R, Haber S, Conney AH. (1970). Effect of enzyme induction on the metabolism and tissue distribution of benzo(alpha)pyrene. Cancer Res 30:2893–7.

Shamoo DA, Johnson TR, Trim SC, et al. (1991). Activity patterns in a panel of outdoor workers exposed to oxidant pollution. J Expo Anal Environ Epidemiol 1:423–38.

St. Charles FK, McAughey J, Shepperd CJ. (2013). Methodologies for the quantitative estimation of toxicant dose to cigarette smokers using physical, chemical and bioanalytical data. Inhal Toxicol 25: 383–97.

Sun JD, Wolff RK, Kanapilly GM. (1982). Deposition, retention, and biological fate of inhaled Benzo[a]pyrene absorbed onto ultrafine particles and as a pure aerosol. Toxicol Appl Pharmacol 65:231–44.

Sun JD, Wolff RK, Kanapilly GM, McClellan R. (1984). Lung retention and metabolic fate of inhaled benzo(a)pyrene associated with diesel exhaust particles. Toxicol Appl Pharmacol 73:48–59.

Thyssen J, Althoff J, Kimmerle G, Mohr U. (1981). Inhalation studies with benzo[a]pyrene in Syrian golden hamsters. J Natl Cancer Inst 66: 575–7.

USEPA. (1994). Methods for derivation of inhalation reference concentrations and application of inhalation dosimetry. US Environmental Protection Agency, Office of Health and Environmental Assessment. EPA/600/8-90/066F.

USEPA. (2005). Guidelines for carcinogen risk assessment. US Environmental Protection Agency. EPA/630/P-03/001F.

USEPA. (2013). Toxicological review of Benzo[a]pyrene (CASRN 50-32-8) in support of summary information on the integrated risk information system (IRIS) (Public comment draft). US Environmental Protection Agency, Office of Research and Development. EPA/635/R13/138a

USEPA. (2011). Exposure factors handbook: 2011 edition. September. United States Environmental Protection Agency, Office of Research and Development, Washington, DC. EPA/600/P-95/002Fa.

Wiersma DA, Roth RA. (1983). Total body clearance of circulating benzo(a)pyrene in conscious rats: effect of pretreatment with 3-methylcholanthrene and the role of liver and lung. J Pharmacol Exp Ther 226:661–7.

Withey JR, Shelden J, Law FCP, Abedini S. (1993). Distribution of benzo[a]pyrene in pregnant rats following inhalation exposure and a comparison with similar data obtained with pyrene. J Appl Toxicol 13:193–202.

Wolff RK, Griffith WC, Henderson RF, et al. (1989). Effects of repeated inhalation exposures to 1-nitropyrene, benzo[a]pyrene, Ga_2O_3 particles, and SO_2 alone and in combinations on particle clearance, bronchoalveolar lavage fluid composition, and histopathology. J Toxicol Env Health 27:123–38.

Xue W, Warshawsky D. (2005). Metabolic activation of polycyclic and heterocyclic aromatic hydrocarbons and DNA damage: a review. Toxicol Appl Pharmacol 206:73–93.